Gas-Phase Reactions of Tantalum Carbide Cluster Ions with Deuterium and Small Hydrocarbons

Carolyn J. Cassady† and Stephen W. McElvany*

Contribution from the Chemistry Division, Code 6111, Naval Research Laboratory, Washington, D.C. 20375-5000. *Received November 1, 1989*

Abstract: The gas-phase ion/molecule reactions of tantalum carbide cluster ions (TaC_y^+, $y = 0$–14) with D_2, CH_4, C_2H_4, and C_2H_6 have been investigated by Fourier transform mass spectrometry. Product branching ratios and reaction rate constants are reported. The addition of tantalum dramatically alters the reactivity relative to that of the corresponding carbon clusters (C_y^+), leading to the conclusion that the TaC_y^+ reactions are initiated on the metal. In addition, the extensive dehydrogenation and secondary reactivity that characterize the reactions of Ta^+ with hydrocarbons are observed for TaC_y^+. Experiments with isotopically labeled precursors were performed, as well as low-energy collision-induced dissociation studies of major reaction products. The implications of these studies with respect to TaC_y^+ structures and reaction mechanisms are discussed. Total scrambling of the labeled carbon occurred during the TaC_y^+ reactions with $^{13}CH_4$. This indicates that the mechanism involves incorporation of the methane carbon into the C_y ligand(s) prior to elimination of a neutral and suggests the possibility of cyclic TaC_y^+ structures. Evidence is also presented for two structural isomers of TaC_7^+, TaC_8^+, and TaC_9^+.

The gas-phase chemistries of carbon cluster ions[1] and transition-metal-containing ions[2] have been the subjects of extensive research in the past few years. Studies of the structures and reactivities of these species are of relevance to several areas of science, including combustion processes, astrochemistry, catalysis, and surface chemistry. The study of gas-phase metal carbide ions is a logical extension of this work. Metal carbides play important roles in materials science and electronics due to their great strengths and high melting points.[3] In addition, they may be intermediates in various organometallic processes, including the Fischer–Tropsch synthesis of hydrocarbons,[4] olefin metathesis,[5] and acetylide catalysis processes.[6]

Numerous Knudsen effusion mass spectrometry studies over the past three decades have involved metal carbide species produced at high temperatures from mixtures of metal powders and graphite.[7-10] These studies have been limited to relatively small metal carbides, $M_xC_y^+$ ($x = 1$ and 2, $y = 1$–8). Similar $M_xC_y^+$ distributions have been obtained by secondary-ion mass spectrometry (SIMS) on bulk metal carbides.[11] Larger monometal carbide ions, MC_y^+ ($y > 40$), have been produced by laser vaporization of metal/graphite samples in a high-pressure supersonic expansion cluster source.[12]

Recently, we reported that tungsten carbide and tantalum carbide cluster ions can be generated by direct laser vaporization (DLV) of metal powder/carbon mixtures in a Fourier transform mass spectrometer (FTMS).[13,14] Tantalum has been the focus of detailed investigation because it is both monoisotopic, which facilitates MS/MS studies, and relatively high in mass (m/z 181), making the TaC_y^+ higher in mass than the abundant low-mass carbon cluster ions (C_y^+, $y < 15$) that are also produced by DLV. DLV of tantalum/carbon yields primarily Ta^+. In addition, a series of tantalum carbide ions, $Ta_xC_y^+$ ($x = 1$–11, $y = 1$–26), are formed, with TaC_2^+ and TaC_4^+ dominating. The TaC_y^+ distribution from DLV is comparable to that seen in Knudsen effusion mass spectrometry experiments with other early transition metals;[7-10] however, the ratio of carbon to metal is much larger with DLV. The similarity with Knudsen cell experiments, as well as the results of DLV experiments with isotopically labeled precursors,[13] suggests that the ions produced by DLV originate from recombination reactions in the laser-generated plasma. The low-energy collision-induced dissociation (CID) of mass-selected $Ta_xC_y^+$ was also discussed in our recent report.[13]

The structures of MC_y species are an intriguing aspect of gas-phase metal carbide chemistry. Although exact structures are unknown, several possibilities are given below with TaC_7^+ as an example. These depictions illustrate the arrangement of atoms and not the nature of bonding. Multiple bonding undoubtedly exists in these species since organometallic complexes of Ta frequently contain double or triple Ta—C bonds[15] and gas-phase carbon clusters contain C=C bonds.[16] Knudsen cell studies have inferred MC_y structures on the basis of the consistency between assumed structures and thermodynamic data obtained from

†NRC/NRL Postdoctoral Research Associate. Current addresss: Department of Chemistry, Miami University, Oxford, OH 45056.

(1) (a) Zhang, Q. L.; O'Brien, S. C.; Heath, J. R.; Liu, Y.; Curl, R. F.; Kroto, H. W.; Smalley, R. E. *J. Phys. Chem.* **1986**, *90*, 525-8. (b) Heath, J. R.; Zhang, Q.; O'Brien, S. C.; Curl, R. F.; Kroto, H. W.; Smalley, R. E. *J. Am. Chem. Soc.* **1987**, *109*, 359-63. (c) Cox, D. M.; Reichmann, K. C.; Kaldor, A. *J. Chem. Phys.* **1988**, *88*, 1588-97. (d) Bloomfield, L. A.; Geusic, M. E.; Freeman, R. R.; Brown, W. L. *Chem. Phys. Lett.* **1985**, *121*, 33-7. (e) Radi, P. P.; Bunn, T. L.; Kemper, P. R.; Molchan, M. E.; Bowers, M. T. *J. Chem. Phys.* **1988**, *88*, 2809-14. (f) McElvany, S. W.; Creasy, W. R.; O'Keefe, A. *J. Chem. Phys.* **1986**, *85*, 632-3. (g) Bohme, D. K.; Włodek, S.; Williams, L.; Forte, L.; Fox, A. *J. Chem. Phys.* **1987**, *87*, 6934-8.

(2) (a) Buckner, S. W.; Freiser, B. S. *Polyhedron* **1988**, *7*, 1583-603. (b) Allison, J.; Mavridis, A.; Harrison, J. F. *Polyhedron* **1988**, *7*, 1559-72. (c) Armentrout, P. B.; Georgiadis, R. *Polyhedron* **1988**, *7*, 1573-81.

(3) (a) Storms, E. K. In *Refractory Materials*; Margrave, J. L., Ed.; Academic Press: New York, 1967; Vol. 2. (b) Silberbach, H.; Merz, H. *Z. Phys. B* **1985**, *59*, 143-9. (c) Gesheva, K.; Vlakhov, E. *Mater. Lett.* **1987**, *5*, 276-9.

(4) (a) Anderson, R. B.; Kōbel, H.; Ralek, M. *The Fischer-Tropsch Synthesis*; Academic Press: New York, 1984. (b) Brady, R. C., III; Pettit, R. *J. Am. Chem. Soc.* **1981**, *103*, 1287-9. (c) Rofer-DePoorter, C. K. *Chem. Rev.* **1981**, *81*, 447-74.

(5) (a) Ivin, K. J. *Olefin Metathesis*; Academic Press: New York, 1983. (b) Calderon, N.; Lawrence, J. P.; Ofstead, E. A. *Adv. Organomet. Chem.* **1979**, *17*, 449-92. (c) Grubbs, R. H. *Comp. Organomet. Chem.* **1982**, *8*, 499-551.

(6) Parshall, G. W. *Homogeneous Catalysis*; Wiley-Interscience: New York, 1980; pp 151-2.

(7) (a) Gupta, S. K.; Kingcade, J. E., Jr.; Gingerich, K. A. *Adv. Mass Spectrom.* **1980**, *8*, 445-51. (b) Gingerich, K. A. *Current Topics in Materials Science*; Kaldis, E., Ed.; North-Holland: Amsterdam, 1980; Vol. 6, pp 347-462.

(8) Pelino, M.; Haque, R.; Bencivenni, L.; Gingerich, K. A. *J. Chem. Phys.* **1988**, *88*, 6534-9.

(9) (a) Gingerich, K. A.; Pelino, M.; Haque, R. *High Temp. Sci.* **1981**, *14*, 137-51. (b) Gingerich, K. A.; Haque, R.; Pelino, M. *J. Chem. Soc., Faraday Trans. 1* **1982**, *78*, 341-6.

(10) Kingcade, J. E., Jr.; Cocke, D. L.; Gingerich, K. A. *High Temp. Sci.* **1983**, *16*, 89-109.

(11) (a) Leleyter, M.; Joyes, P. *Surf. Sci.* **1985**, *156*, 800-13. (b) Leleyter, M.; Ortoli, S.; Joyes, P. *Surf. Sci.* **1981**, *106*, 293-300.

(12) (a) Heath, J. R.; O'Brien, S. C.; Zhang, Q.; Liu, Y.; Curl, R. F.; Kroto, H. W.; Tittel, F. K.; Smalley, R. E. *J. Am. Chem. Soc.* **1985**, *107*, 7779-80. (b) Weiss, F. D.; Elkind, J. L.; O'Brien, S. C.; Curl, R. F.; Smalley, R. E. *J. Am. Chem. Soc.* **1988**, 110, 4464-5. (c) Cox, D. M.; Trevor, D. J.; Reichmann, K. C.; Kaldor, A. *J. Am. Chem. Soc.* **1986**, *108*, 2457-8.

(13) McElvany, S. W.; Cassady, C. J. *J. Phys. Chem.* **1990**, *94*, 2057-62.

(14) McElvany, S. W.; Ross, M. M.; Baronavski, A. P. *Anal. Inst.* **1988**, *17*, 23-40.

(15) (a) Schrock, R. R. *J. Am. Chem. Soc.* **1976**, *98*, 5399-400. (b) Schrock, R. R.; Sharp, P. R. *J. Am. Chem. Soc.* **1978**, *100*, 2389-98. (c) Schrock, R. R. *Acc. Chem. Res.* **1979**, *12*, 98.

(16) McElvany, S. W.; Dunlap, B. I.; O'Keefe, A. *J. Chem. Phys.* **1987**, *86*, 715-25.

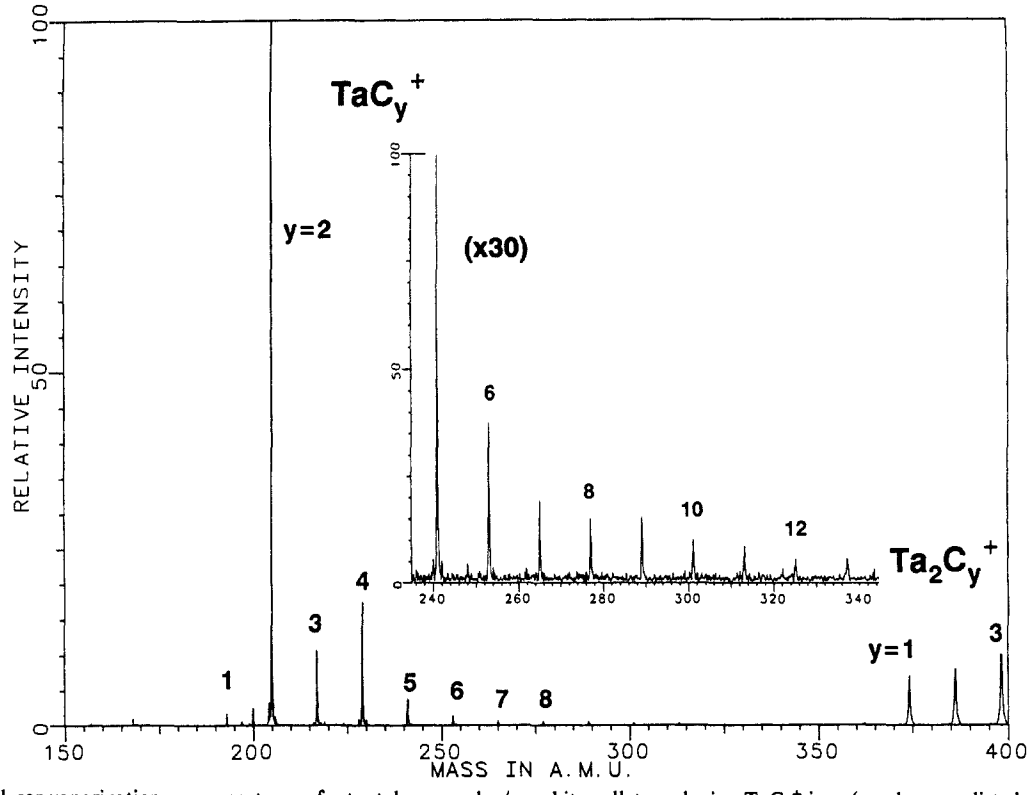

Figure 1. Direct laser vaporization mass spectrum of a tantalum powder/graphite pellet producing TaC_y^+ ions (y values are listed above the peaks). Ta^+ was ejected during the ionization event.

equilibrium measurements as a function of temperature.[7-10] This work has included larger monometal carbides (e.g., YC_y,[8] LaC_y,[9] and CeC_y,[10] $y \leq 8$, 8, and 6, respectively), but TaC_y species have not been investigated. These studies suggest that MC_y consist of linear (or possibly bent) carbon chains with the metal attached at one end, that is, structure I for Ta^+. In addition, small

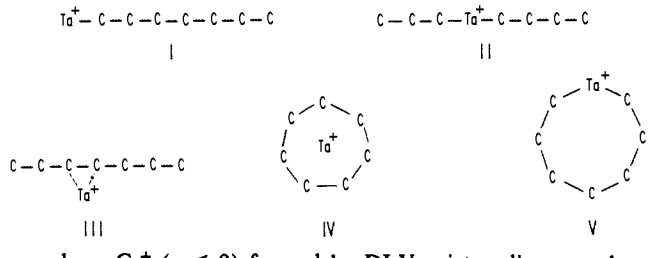

I II III IV V

gas-phase C_y^+ ($y \leq 9$) formed by DLV exist as linear carbon chains,[16-18] and metallocumulene species are known to exist in solution.[19] The Knudsen cell work also suggests that multiple ligand structures (II) are only important for MC_4, which may have a dicarbide structure (C_2-M-C_2), and that metal attachment at an internal position on the carbon chain (III) is not a preferred configuration.[7-10] Cyclic structures were not appraised in the Knudsen cell work; however, the current ion/molecule reaction studies and our previous low-energy CID investigations of TaC_y^+[13] provide evidence for their existence. Metallocene structures (IV) are plausible since laser vaporization produces C_y^+ with cyclic structures for $y \geq 10$ and both cyclic and linear structures for y = 7-9.[18] In addition, C_{10} loss is a major low-energy CID pathway for TaC_y^+ ($y \geq 10$) and may indicate the presence of an intact cyclic C_{10} ligand.[13] Metallacycle structures (V) are another possibility, particularly for $y \geq 5$ because cyclic C_y^+ are known for $y \geq 7$[16-18] and Ta is roughly equal in size to a C=C unit. Also, metallacycle Ta compounds have been observed in solution.[20]

This paper presents the first studies on the gas-phase reactivities of metal carbide cluster ions, TaC_y^+ (y = 1-14), with several small molecules (D_2, CH_4, C_2H_4, C_2H_6). Tantalum has a rich organometallic chemistry in solution, particularly with regard to the formation of metal-alkylidene and -alkylidyne species.[15] The current work indicates that gas-phase organotantalum chemistry is equally complex. The chemistries of the bare metal ion, Ta^+,[21] and the corresponding carbon clusters, C_y^+,[16,17] are compared to that of TaC_y^+. Isotopically labeled reactants are used to gain insight on reaction mechanisms and TaC_y^+ structures.

Experimental Section

All experiments were performed with a Fourier transform ion cyclotron resonance mass spectrometer,[22] which has previously been described in detail.[18] The mass spectrometer consists of a Nicolet FTMS/1000 data system and a Nicolet 3-T superconducting magnet. The trapping plates of the 1 in. × 1 in. × 2 in. (z-axis) rectangular trapping cell are composed of 90% transparent nickel mesh. This allowed the frequency-doubled output of a Quanta-Ray DCR-2 Nd:YAG laser (532 nm, 1-5 mJ/pulse) to traverse the cell and vaporize the sample that was placed on a solids probe and inserted flush with one of the trapping plates.

TaC_y^+ were formed by laser vaporization of pellets containing tantalum powder (325 mesh, Johnston Matthey) mixed with either graphite (325 mesh, Alfa Inorganics), amorphous ^{12}C (99.9% Isotec Inc.) or amorphous ^{13}C (>99.0%, Isotec). A molar ratio of ~1 Ta to 4 C was typically employed. Production of TaC_y^+ from Ta/carbon pellets has been discussed previously.[13] A representative mass spectrum of TaC_y^+ obtained from Ta/graphite is shown in Figure 1. TaC_y^+ generated by DLV may have a wide range of internal energies. However, aside from instances noted in the text, appreciable pressure effects (i.e., collisional cooling) during the reactions were not observed, suggesting that the ions are predominantly in their ground state.

(17) McElvany, S. W. *J. Chem. Phys.* **1988**, *89*, 2063-75.
(18) Parent, D. C.; McElvany, S. W. *J. Am. Chem. Soc.* **1989**, *111*, 2393-401.
(19) (a) Mayr, A.; Schaefer, K. C.; Huang, E. Y. *J. Am. Chem. Soc.* **1984**, *106*, 1517-8. (b) Birdwhistell, K. R.; Templeton, J. L. *Organometallics* **1985**, *4*, 2062-4. (c) Höhn, A.; Otto, H.; Dziallas, M.; Werner, H. *J. Chem. Soc. Chem. Commun.* **1987**, 852-4.
(20) (a) Rocklage, S. M.; Fellmann, J. D.; Rupprecht, G. A.; Messerle, L. W.; Schrock, R. R. *J. Am. Chem. Soc.* **1981**, *103*, 1440-7. (b) Wallace, K. C.; Dewan, J. C.; Schrock, R. R. *Organometallics* **1986**, *5*, 2162-4.
(21) Buckner, S. W.; MacMahon, T. J.; Byrd, G. D.; Freiser, B. S. *Inorg. Chem.* **1989**, *28*, 3511-8.
(22) A recent review of FTMS appears in *Fourier Transform Mass Spectrometry: Evolution, Innovation, and Applications*; Buchanan, M. V., Ed.; ACS Symposium Series 359; American Chemical Society: Washington, DC, 1987.

Table I. Branching Ratios and Normalized Rate Constants for the Primary Reactions of TaC_y^+ and D_2

	cluster size (y)														
products	0	1	2	3	4	5	6	7	8	9	10	11	12	13	14
$TaC_yD_2^+$	NR[a]				NR[a]				1.00	1.00	1.00	1.00	1.00	1.00	1.00
$TaC_yD^+ + D$		1.00		1.00											
$TaC_{y-2}^+ + C_2D_2$			1.00			1.00	1.00	1.00							
normalized rate const (k_p)	<0.001	1.00[b]	0.30	0.048	<0.001	0.0015[c]	0.26	0.069[c]	0.23[d]	0.069[c]	0.66	0.013	0.0018[c]	0.0041[c]	0.015[c]

[a] NR indicates that this ion did not undergo any reactions. [b] The absolute rate constant for the reaction of TaC^+ was estimated to be 5.3×10^{-10} cm^3/s. [c] See the text for explanation. [d] Rate constant for the reactive fraction of TaC_8^+ as discussed in the text.

Following TaC_y^+ formation, ions corresponding to a specific cluster size were isolated in the FTMS cell with resonance frequency ejection techniques.[23] The mass-selected ions were allowed to react with a static pressure of reactant gas maintained at pressures up to 1×10^{-6} Torr, with typical operating pressures of $(1-5) \times 10^{-7}$ Torr. For H/D exchange reactions,[24] the reactant ions were formed by reactions of TaC_y^+ with a hydrocarbon reagent gas introduced into the vacuum chamber via a General Valve Corp. Series 9 pulsed solenoid valve.[25] The pulse pressure reached a maximum of 10^{-5} Torr and was pumped away by an Edwards Diffstak Series 160 diffusion pump within ~400 ms. In cases noted in the text, the pulsed valve was also used to admit xenon buffer gas. Collision-induced dissociation (CID) experiments[26] employed a static pressure of xenon collision gas on the order of $(1-5) \times 10^{-6}$ Torr. The collision energy was varied from 0 to 100 eV (laboratory).

The primary product ion branching ratios listed in Tables I–VII are reproducible to ±10%. Rate constants were determined by observing the pseudo-first-order change in reactant ion intensity as a function of time at a constant pressure. All reactions were studied to greater than 80% completion except for cases of prohibitively slow reaction or low reactant ion intensity. Except as noted in the text, all first-order decay plots were linear, suggesting the predominance of ground-state reactant ions. Pressures were measured with a calibrated ion gauge[27] and corrected for reactant gas ionization efficiency.[28] Errors in the pressure calibration factor and from other sources may render the absolute rate constants in error by as much as a factor of 2–3. Differences in relative rate constants should be significant, however, since they were measured under similar conditions.

Results and Discussion

Deuterium Reactions. Reaction Products and Rates. Primary products, branching ratios, and rate constants for the ion/molecule reactions of TaC_y^+ with D_2 are listed in Table I. Deuterium was used in these studies, rather than H_2, to avoid nominal mass overlap between potential products and reactant ions containing naturally occurring ^{13}C (e.g., TaC_yH^+ and $TaC_{y-1}{}^{13}C^+$). TaC_y^+ undergo reactions 1–3 with D_2. In contrast, the pure carbon cluster

$$TaC_y^+ + D_2 \rightarrow TaC_yD_2^+ \quad y = 8\text{–}14 \qquad (1)$$

$$\rightarrow TaC_yD^+ + D \quad y = 1, 3 \qquad (2)$$

$$\rightarrow TaC_{y-2}^+ + C_2D_2 \quad y = 2, 5\text{–}7 \qquad (3)$$

ions, C_y^+ (y = 3–9), react exclusively by D elimination (reaction 4) with the exception of C_6^+ and C_8^+, which also eliminate C_3

$$C_y^+ + D_2 \rightarrow C_yD^+ + D \quad y = 3\text{–}9 \qquad (4)$$

$$\rightarrow C_{y-3}D_2^+ + C_3 \quad y = 6, 8 \qquad (5)$$

(reaction 5) at 15% and 25%, respectively.[16] Several studies suggest that the C_y^+ reactions occur at carbene sites on the ends of linear chains (VI).[16-18] The dramatic difference in TaC_y^+ and

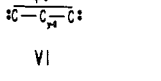

VI

VII

C_y^+ reactivity with D_2 indicates that Ta is playing an active role in the TaC_y^+ reactions. These processes presumably involve metal insertion into the D–D bond, resulting in the formation of intermediate VII. This may be followed by ligand rearrangement on Ta and elimination of neutral molecules or radicals.

Formation of the stable neutral C_2D_2 (reaction 3) is surprising because the reactions of Ta^+ with hydrocarbons involve almost exclusive dehydrogenation.[21] The presence of this exothermic reaction for y = 2 and 5–7 indicates that $\Delta H_f(TaC_y^+)$ is at least 54 kcal/mol greater than $\Delta H_f(TaC_{y-2}^+)$.[29] C_y^+ do not undergo C_2D_2 loss, and this process is not expected to be exothermic since MNDO calculations indicate that for y = 5–9 $\Delta H_f(C_y^+)$ is only 29–42 kcal/mol greater than $\Delta H_f(C_{y-2}^+)$.[16] The observation of reaction 3 for TaC_2^+ yields an upper limit of $D(Ta^+–C_2) < 145$ kcal/mol.[29]

TaC^+ and TaC_3^+ react with D_2 in a manner similar to that of C_y^+ (y = 3–9), undergoing D elimination (reaction 2). In both cases the primary product ion reacts further with D_2 to form $TaC_yD_2^+$, reaction 6. An analogous process occurs for C_yD^+ (y = 3, 4, 6, 8).[16] Elimination of D may be the only exothermic pathway available to TaC^+ and TaC_3^+. For TaC^+, loss of CD_2 to generate Ta^+ is not exothermic if $D(Ta^+–C) > 78$ kcal/mol.[29] This is almost certainly the case, since for the other group 5 metals $D(V^+–C) = 88 \pm 5$ kcal/mol[30] and $D(Nb^+–C) > 138$ kcal/mol.[31] For TaC_3^+, C_2D_2 elimination will only occur if the $Ta^+–C$ bond is at least 25 kcal/mol stronger than the $Ta^+–C_3$ bond.[29] While no absolute bond strengths are available for $Ta^+–C_y$, Knudsen cell studies involving other early transition metals have found that the M–C bond is weak relative to $M–C_2$ and $M–C_3$.[7-10] Further evidence for a weak $Ta^+–C$ bond is seen in the DLV mass spectra of Ta/carbon mixtures (Figure 1), where TaC^+ is formed in very low abundance relative to TaC_y^+ (y = 2–4).[13]

$$TaC_yD^+ + D_2 \rightarrow TaC_yD_2^+ + D \quad y = 1, 3 \qquad (6)$$

The absence of TaD^+ formation from Ta^+ and D_2 indicates that $D(Ta^+–D) < 106$ kcal/mol.[29] This is not surprising since no bare atomic metal ion is known to react exothermically with D_2. However, the nonreactivity of TaC_4^+ is unexpected, because this ion readily reacts with the other small molecules in this study. As discussed earlier, Knudsen cell studies suggest that MC_4 has a dicarbide structure (II) while other MC_y species involve metal attachment at a linear carbon chain (I). In addition, Knudsen cell investigations of larger metal carbides (YC_y,[8] LaC_y,[9] and CeC_y,[10] y = 2–6) reveal that $\Delta H_f(MC_y)$ increases by 15–40 kcal/mol with the addition of each successive carbon. Only $\Delta H_f(MC_4)$, which is within ±4 kcal/mol of $\Delta H_f(MC_3)$, does not follow this trend; this is probably a result of MC_4 having a structure different from that of other MC_y. Thus, it is possible that TaC_4^+ has a dicarbide structure, $C_2–Ta^+–C_2$, and cannot undergo reaction 2, which is endothermic if $\Delta H_f(TaC_4^+) - \Delta H_f(TaC_2^+) < 54$ kcal/mol.[29]

Larger TaC_y^+ (y = 8–14) react with D_2 only through association reaction 1. For y = 9 and 11–14, these reactions are a factor of 10^2–10^3 slower than the Langevin collision rate[32] of 1.1×10^{-9}

(23) Comisarow, M. B.; Grassi, V.; Parisod, G. *Chem. Phys. Lett.* **1978**, *57*, 413–6.
(24) (a) Jacobson, D. B.; Freiser, B. S. *J. Am. Chem. Soc.* **1985**, *107*, 72–80. (b) Cassady, C. J.; Freiser, B. S. *J. Am. Chem. Soc.* **1985**, *107*, 1566–73.
(25) Carlin, T. J.; Freiser, B. S. *Anal. Chem.* **1983**, *55*, 571–4.
(26) Cody, R. B.; Freiser, B. S. *Int. J. Mass Spectrom. Ion Phys.* **1982**, *41*, 199–204.
(27) The ion gauge was calibrated with the reaction $Kr^+ + CO_2 \rightarrow Kr + CO_2^+$, with rate constant information obtained from: Ikezoe, Y.; Matsuoka, S.; Takebe, M.; Viggiano, A. *Gas Phase Ion-Molecule Reaction Rate Constants through 1986*; Maruzen: Tokyo, 1987.
(28) Bartmess, J. E.; Georgiadis, R. M. *Vacuum* **1983**, *33*, 149–53.
(29) Except as noted, supplementary thermochemical information was obtained from: Lias, S. G.; Bartmess, J. E.; Liebman, J. F.; Holmes, J. L.; Levin, R. D.; Mallard, W. G. *J. Phys. Chem. Ref. Data* **1988**, 17 (Suppl. 1).
(30) Aristov, N.; Armentrout, P. B. *J. Am. Chem. Soc.* **1984**, *106*, 4065–6.
(31) Hettich, R. L.; Freiser, B. S. *J. Am. Chem. Soc.* **1987**, *109*, 3543–8.

Table II. Branching Ratios for the Low-Energy Collision-Induced Dissociation of $TaC_yH_2^+$

	cluster size (y)										
products	1	2	3	4	5	6	7	8	9	10	11
$TaC_yH^+ + H$	0.42[a]									0.10	
$TaC_y^+ + H_2$			0.45		0.21					0.16	
$TaC_{y-2}^+ + C_2H_2$		*b*			0.59	1.00	0.74			0.12	0.38
$TaC_{y-4}^+ + C_4H_2$				*b*			0.26	1.00	1.00		
$TaC_{y-6}^+ + C_6H_2$										0.52	0.62
$Ta^+ + C_yH_2$	0.58	1.00	0.55	1.00	0.20					0.10	

[a] Reported branching ratios were obtained with collision energies of 40–50 eV (laboratory). [b] This pathway is observed, producing $Ta^+ + C_yH_2$.

cm^3/s. These rates were measured at pressures of $\sim 10^{-6}$ Torr, where the average time between collisions is ~28 ms. Therefore, it is possible that collisional stabilization plays a role in adduct formation for these ions. TaC_8^+ and TaC_{10}^+, however, react with $k_{obsd}/k_{Langevin}$ ratios of 0.3 and 0.1, respectively. Here, adduct formation is independent of pressure and occurs readily even at D_2 pressures of 2.2×10^{-7} Torr where the average time between collisions is 128 ms. These results suggest that stabilizing collisions with D_2 are not necessary for the formation and detection of $TaC_8D_2^+$ and $TaC_{10}D_2^+$. Therefore, these reactions may involve radiative association. Radiative association is also postulated in the reactions of C_y^+ with HCN,[18] C_2H_2, and C_2H_4.[17]

In addition to adduct formation, minor amounts (<10%) of lower mass products were periodically observed for TaC_y^+ (y = 8, 9, 11). The abundances of these species decreased with increasing pressure, including a pulsed xenon pressure applied prior to reaction. Similar phenomena were seen in the reactions with hydrocarbons. CID studies revealed that these ions are also produced as the lowest energy fragmentation pathways of the adducts. Thus, a fraction of TaC_y^+ contains sufficient excess internal energy that when not removed by collisions, results in dissociation of the adduct. Low-energy CID studies of $TaC_yH_2^+$ produced by reactions with D_2, CH_4, or C_2H_4 are summarized in Table II. The method of $TaC_yH_2^+$ generation had only negligible effects on the CID data, suggesting that $TaC_yH_2^+$ produced from different precursors have the same structures. Interestingly, $TaC_yH_2^+$ dissociate to eliminate C_yH_2 with even y, while the major TaC_y^+ CID pathways involve C_3, C_5, and C_{10} elimination.[13] These differences may result from the energetics of the dissociation reactions because C_yD_2, with even y, have considerably lower heats of formation[29] (i.e., are more stable) than C_y.

At longer reaction times, the primary product ions from reaction 1 that contain an odd number of carbons undergo secondary association reactions with D_2. For y = 9, 11, and 13, $TaC_yD_8^+$ is produced from the association of four D_2 molecules. These subsequent reactions occur at rates near or greater than that of the primary reaction. In contrast, $TaC_yD_2^+$ (y = 8, 10, 12, 14) do not readily react further. The variation in secondary reactivity between ions with odd and even numbers of carbons may be due to thermodynamic differences since neutral C_yD_2 are only known to be stable when y is even.[29] Therefore, C_yD_2 ligands with odd y may undergo facile hydrogenations to generate more stable ligands.

The rate constants for the primary reactions of TaC_y^+ with D_2, normalized by the rate constant for TaC^+, are plotted versus cluster size in Figure 2. Except for the nonreactivity of Ta^+ and TaC_4^+, the rate trends exhibited with D_2 are also found in TaC_y^+ reactions with CH_4 and C_2H_6. TaC^+ reacts the fastest, suggesting that a relatively weak Ta^+–C bond increases the reaction exothermicity. TaC_y^+ (y = 5–14) with an even number of carbons react faster than neighboring ions with an odd number of carbons. This contrasts with the reactions of C_y^+ with D_2[16] and small hydrocarbons,[17] where odd clusters react faster than even clusters. In general, experimental studies of C_y^+ and C_yX^+ (X = H, D, O, CN) suggest that, for odd electron series, odd y ions will be more reactive than even y ions, and vice versa, regardless of the neutral reactant.[16-18] This is consistent with Hückel theory but is only

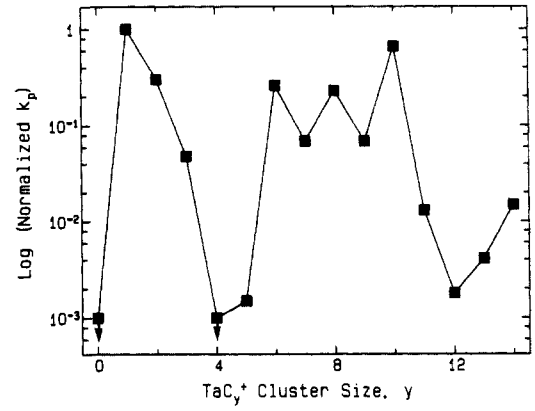

Figure 2. Semilog plot of the rate constants for the primary reactions of TaC_y^+ with D_2, normalized to the rate constant for y = 1, versus cluster size y. Arrows on the squares indicate that these values are upper limits (i.e., no reaction was observed).

applicable to linear molecules.[11,18] TaC_y^+, which are even electron species, follow this trend; however, it is not clear that a meaningful comparison can be made. The mechanism of TaC_y^+ reactions undoubtedly involves Ta d orbitals and is quite different from that of C_y^+ and C_yX^+. Also, the existence of TaC_y^+ as linear molecules (I) is dubious, particularly for larger y. In fact, the TaC_y^+ odd–even rate trend may imply the presence of metallacycle structures (V). Metallacycles can be envisioned as consisting of cumulene- and polyacetylene-type resonance structures. For TaC_y^+ with even y (VIII and IX), a polyacetylene-type structure

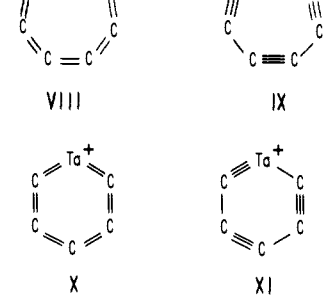

(IX) results in two nonbonding electrons on Ta^+, which may facilitate bonding at the metal center in the initial ion/molecule complex. TaC_y^+ with odd y do not have resonance structures with nonbonding electrons (X and XI) and, as a consequence, may react more slowly.

A dramatic decrease in reaction rate with D_2 occurs between TaC_{10}^+ and TaC_{11}^+. A sharp drop in the rate of reaction with D_2 exists between C_9^+ and C_{10}^+ and is believed to be the result of a change in structure from linear chains to monocyclic rings.[16] The reason for the reactivity decrease between TaC_{10}^+ and TaC_{11}^+ is less clear. One possibility is that for TaC_y^+ ($y \geq 11$) Ta^+ resides in the center of a planar monocyclic ring of carbons. Such a structure should lead to maximum bonding between Ta^+ and C_y, resulting in coordinative saturation of Ta^+ and a notable decrease in reactivity. Another explanation is that a change in the extent of charge delocalization occurs between TaC_{10}^+ and TaC_{11}^+. For reactions with C_2H_2 and C_2H_4, a large decrease in rate exists

(32) Calculated from the Langevin equation with polarizabilities obtained from: Miller, K. J.; Savchik, J. A. *J. Am. Chem. Soc.* **1979**, *101*, 7206–13.

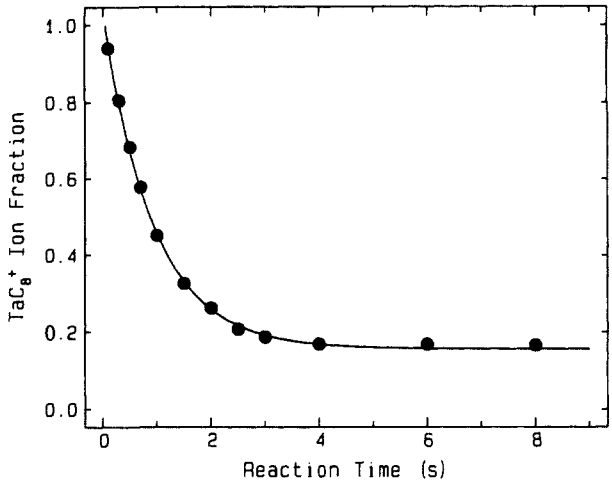

Figure 3. Reactant loss curve for the reaction of TaC_8^+ with D_2. The curve represents a nonlinear least-squares fit of the data to the sum of an exponential and a constant. Error bars (2σ) are smaller than the point size. Approximately 84% of the TaC_8^+ reacts with D_2.

between C_{10}^+ and C_{11}^+ and has been attributed to a decrease in the ionization potential[17] (IP(C_{10}) = 9.1 eV[33] and IP(C_{11}) = 7.4 eV[33]). Ta has an ionization potential of 7.4 eV; therefore, it is probable that extensive charge delocalization occurs for TaC_{11}^+ compared to TaC_{10}^+ and may be sufficient to account for a decrease in the rate of reaction.

Multiple Structural Isomers. TaC_8^+ exhibits only partial reactivity with D_2. While 84% of the ion population readily undergoes association reaction 1, the remaining 16% does not react. The reaction of TaC_8^+ with D_2 as a function of time is illustrated in Figure 3. Similar behavior is seen with CH_4 and C_2H_6. The percentage of unreactive ions remained constant as a function of D_2 pressure (0.2–1.0) $\times 10^{-6}$ Torr) for times up to 8 s and was not affected by application of a pulsed pressure of nonreactive collision gas (xenon at $\sim 10^{-5}$ Torr) immediately following TaC_8^+ formation and isolation. This suggests that the observed kinetic behavior is not the result of excited ions. Thus, the data lead to the conclusion that multiple structural isomers of TaC_8^+ exist. Reactions of C_y^+ (y = 7–9) have also revealed reactive and nonreactive ion populations that have been attributed to linear and cyclic forms of C_y^+, respectively.[16-18] As discussed below, while TaC_7^+ and TaC_9^+ both react to completion with D_2, these reactions exhibit kinetic behavior that may result from multiple structural isomers. Therefore, one interpretation of the TaC_8^+ data is that reactive ions have a linear C_8 ligand (I), while nonreactive ions have a cyclic C_8 ligand (IV or V). Other possibilities are that nonreactive TaC_8^+ contains two C_4 ligands (since TaC_4^+ is also unreactive with D_2) or exists as $Ta(C_2)_4^+$, with four C_2 ligands resulting in coordinative saturation of Ta^+ (which has four valence electrons).

Reactions of TaC_y^+ (y = 5, 12–14) with D_2 have rates on the order of 10^{-11}–10^{-12} cm^3/s, which are slow relative to the Langevin collision rate[32] of 1.1 $\times 10^{-9}$ cm^3/s. These reactions were not monitored to complete disappearance of reactants due to slow rates and low ion intensities. Therefore, while there is no evidence for multiple ion populations, the possibility cannot be ruled out.

TaC_7^+ reacts slowly, but completely, with D_2. Figure 4 illustrates reactant and product ion relative abundances as a function of trapping time with 2.0 $\times 10^{-7}$ Torr of D_2 with (a) no buffer gas and (b) xenon added to 1.3 $\times 10^{-6}$ Torr. The solid lines are biexponential fits for the reactant ion intensity data. Between 0.5- and 2-s reaction time, data lie above the fitted line, giving the curves a "humped" appearance. This hump is pressure-dependent, becoming more pronounced with both increasing buffer gas and reactant pressures. The addition of a pulsed pressure of xenon ($\sim 10^{-5}$ Torr) prior to reaction with D_2 has a negligible effect, suggesting that this behavior is not the result of excited-state

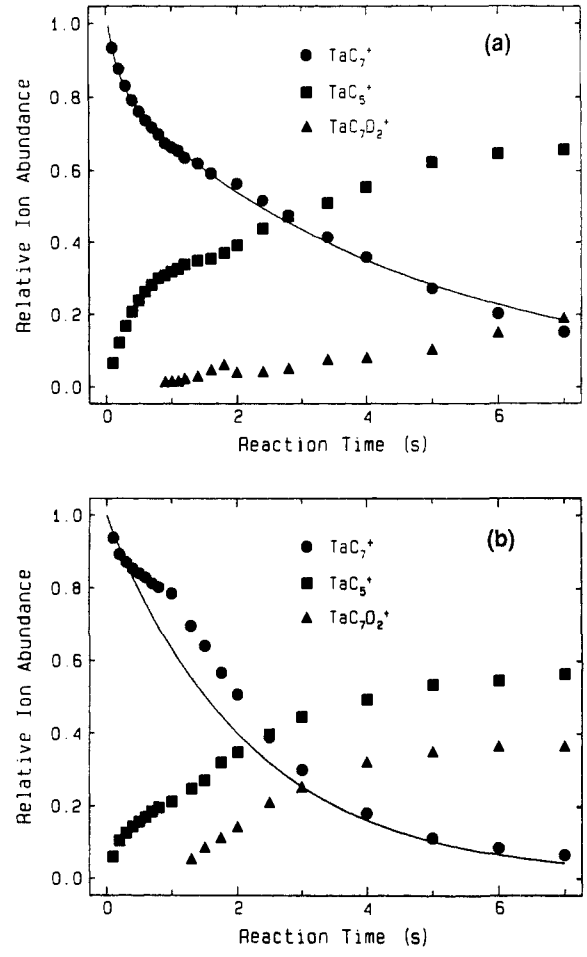

Figure 4. Reactant and product ion intensities as a function of trapping time for the reaction of TaC_7^+ with D_2 (2.0 $\times 10^{-7}$ Torr) with (a) no buffer gas and (b) xenon added to a total pressure of 1.3 $\times 10^{-6}$ Torr. The curve on the TaC_7^+ data represents a nonlinear least-squares fit of the data to the sum of two exponentials. Note the "hump" around reaction times of 1 s.

ions. Aside from the hump, the data at low pressures yield a reasonable fit to a single-exponential function, although fits of slightly better quality can be obtained via a biexponential function (i.e., two ion populations). The low-pressure data (Figure 4a) suggest that the major TaC_7^+ population accounts for ~85% of the ions and reacts at a rate that is roughly a factor of 5 slower than the reaction rate of the minor population. The relative rate constant in Table I is an average value calculated with single-exponential fits of data obtained at several pressures.

At short reaction times, TaC_7^+ and D_2 produce only TaC_5^+ (reaction 2). However, as the reaction time (and thus the number of collisions) increases, association reaction 1, producing $TaC_7D_2^+$, becomes an important process. As can be seen from Figure 4, and particularly Figure 4b, the appearance of the hump in TaC_7^+ abundance corresponds to the initial appearance of $TaC_7D_2^+$ as a product. The hump is actually an indication of a change in rate. With addition of xenon buffer gas at 1.3 $\times 10^{-6}$ Torr (Figure 4b) the hump peaks (and $TaC_7D_2^+$ formation begins) at 1 s. Under these conditions, reactions occur at a rate of $\sim 3 \times 10^{-11}$ cm^3/s for times of 1 s or less and $\sim 9 \times 10^{-11}$ cm^3/s after 1 s. The rate of TaC_5^+ formation is not changing; instead this increased rate is entirely due to the emergence of the association pathway. At a total pressure of 1.3 $\times 10^{-6}$ Torr, the average time between collisions is 23 ms (as opposed to 148 ms at 2.0 $\times 10^{-7}$ Torr). Therefore, at 1.3 $\times 10^{-6}$ Torr the increased collision rate may lead to stabilization of $TaC_7D_2^+$, which at lower pressures would dissociate to primarily regenerate TaC_7^+ and produce minor amounts of TaC_5^+.

The 1-s delay before formation of $TaC_7D_2^+$ may indicate that multiple collisions are necessary to generate the stabilized adduct.

(33) Bach, S. B. H.; Eyler, J. R. *J. Chem. Phys.* **1990**, *92*, 358–63.

Table III. Branching Ratios and Normalized Rate Constants for the Primary Reactions of TaC_y^+ and CH_4

	cluster size (y)														
products	0	1	2	3	4	5	6	7	8	9	10	11	12	13	14
$TaC_{y+1}H_2^+ + H_2$	1.00	0.71	1.00	0.55	0.33		0.13	0.13	0.09		0.08				
$TaC_{y-1}H_2^+ + C_2H_2$				0.45	0.67	1.00	0.87	0.87	0.91	1.00	0.92	1.00	1.00	1.00	1.00
$Ta^+ + C_2H_4$		0.29													
normalized rate const (k_p)	1.00[a]	1.66	0.86	0.28	0.19	0.056[b]	0.48	0.25[b]	1.11[c]	0.12[b]	0.65	0.0061	0.019[b]	0.0073[b]	0.073[b]

[a] The absolute rate constant for the reaction of Ta^+ was estimated to be 3.0×10^{-10} cm^3/s. [b] See text for explanation. [c] Rate constant for the reactive fraction of TaC_8^+ as discussed in the text.

Table IV. Branching Ratios for the Loss of $^{12}C^{13}CH_2$ and $^{12}C_2H_2$ in the Reactions of $Ta^{12}C_y^+$ and $^{13}CH_4$

	cluster size (y)											
products	3	4	5	6	7	8	9	10	11	12	13	14
$Ta^{12}C_{y-1}H_2^+ + {}^{12}C^{13}CH_2$												
exptl	0.51	0.43	*b*	0.32	0.27	0.24	0.32	0.19	*b*	0.23	*b*	0.18
stat[a]	0.50	0.40	0.33	0.29	0.25	0.22	0.20	0.18	0.17	0.15	0.14	0.13
$Ta^{12}C_{y-2}{}^{13}CH_2^+ + {}^{12}C_2H_2$												
exptl	0.49	0.57	*b*	0.68	0.73	0.76	0.68	0.81	*b*	0.77	*b*	0.82
stat[a]	0.50	0.60	0.67	0.71	0.75	0.78	0.80	0.82	0.83	0.85	0.86	0.87

[a] Statistical calculations of branching ratios assume that all carbons have an equal probability of being incorporated in the neutral C_2H_2. The statistical abundance of $Ta^{12}C_{y-1}H_2^+$ is $2/(y+1)$ and of $Ta^{12}C_{y-2}{}^{13}CH_2^+$ is $(y-1)/(y+1)$. [b] For TaC_y^+ (y = 5, 11, 13), the $^{13}CH_4$ reaction is slow relative to the reaction with background water (which forms $Ta^{12}C_{y-1}H_2^+$), preventing the determination of accurate branching ratios for these ions.

It is also possible that two or more TaC_7^+ isomers exist. One isomer, TaC_{7A}^+, may undergo reaction 7 with ~3% of its collisions

$$TaC_{7A}^+ + D_2 \rightarrow TaC_5^+ + C_2D_2 \quad (7)$$

$$TaC_{7A\text{ or }7B}^+ + D_2\ (+Xe) \rightarrow TaC_{7C}^+ + D_2\ (+Xe) \quad (8)$$

$$TaC_{7C}^+ + D_2 \rightarrow TaC_7D_2^+ \quad (9)$$

with D_2 producing TaC_5^+ ($k_{obsd}/k_{Langevin} = 0.03$), while a second isomer, TaC_{7C}^+, forms a stable adduct via reaction 9. In this scenario, TaC_{7C}^+ is not initially produced by DLV but results from structural rearrangement of either TaC_{7A}^+ or another isomer TaC_{7B}^+ following collisions with D_2 or xenon (reaction 8). A similar mechanism has been proposed to explain nonlinear kinetic behavior, including a hump, exhibited during the reactions of C_7^+ with HCN.[18] Reactions of C_7^+ with several small molecules have revealed two isomers: a linear species that reacts rapidly and a cyclic species that is slower to react.[16-18] In addition, the reactions of TaC_7^+ with CH_4 and C_2H_6 suggest the existence of multiple structural isomers, as discussed later in this paper.

TaC_9^+ and possibly TaC_{11}^+ also do not follow single-exponential first-order kinetics in their reactions with D_2. These species are difficult to study since they are initially formed in low abundance by DLV. However, the data appear to decay biexponentially (and without a hump) and imply the existence of two ion populations with rate constants differing by less than a factor of 5. These ions undergo only association reaction 1.

Methane Reactions. Primary Reactions with $^{12}CH_4$. As shown in Table III, TaC_y^+ (y = 0–14) react with CH_4 via primarily two pathways. Dehydrogenation, reaction 10, leads to an increase in

$$TaC_y^+ + CH_4 \rightarrow TaC_{y+1}H_2^+ + H_2 \quad (10)$$

$$TaC_y^+ + CH_4 \rightarrow TaC_{y-1}H_2^+ + C_2H_2 \quad (11)$$

the number of carbon atoms attached to Ta and dominates for smaller TaC_y^+ (y = 0–3). Acetylene elimination, reaction 11, results in a smaller number of carbons in the cluster ion and becomes more abundant as y increases. This is the only process observed for $y \geq 11$. A third channel, generation of Ta^+ by reaction 12, is only observed for TaC^+ and sets an upper limit

$$TaC^+ + CH_4 \rightarrow Ta^+ + C_2H_4 \quad (12)$$

of $D(Ta^+-C) < 141$ kcal/mol.[29] Therefore, based on the D_2 and CH_4 data, this bond energy is bracketed at 78 kcal/mol $< D(Ta^+-C) < 141$ kcal/mol.

The gas-phase reactions of Ta^+ with alkanes, which have been studied in detail by Freiser and co-workers[21] involve primarily cleavage of C–H bonds. This is consistent with numerous gas-phase studies that have shown that metal ions early in the transition series and in the second and third rows preferentially activate C–H bonds (as opposed to C–C bonds).[34-36] In the present work, the reactions of Ta^+ with CH_4 and C_2H_6 were reinvestigated to allow comparison of Ta^+ and TaC_y^+ data obtained under the same experimental conditions. The results of the current study are in agreement with the previous report. Ta^+[21] and Os^+[37] are the only ground-state atomic metal ions that are known to react exothermically with CH_4. Dehydrogenation is the lone process observed and indicates that $D(Ta^+-CH_2) > 111$ kcal/mol.[29]

While TaC_y^+ reacts with CH_4 by primarily two pathways, linear C_y^+ (y = 3–9) undergo five different reactions with CH_4 resulting in the elimination of H, H_2, CH_3, C_2H_2, and C_4H_2. Cyclic C_y^+ (y = 10–19) do not react with CH_4.[17] This difference in reactivity is further indication that Ta is actively involved in the TaC_y^+ reactions.

The reactivity of TaC_y^+ (y = 7–9) with CH_4 is consistent with the D_2 results and provides additional evidence for multiple structural isomers. The remaining TaC_y^+ (y = 0–6, 10–14) react to yield linear pseudo-first-order decay plots, suggesting that only one structural isomer of these species is formed by DLV. Only 85% of the TaC_8^+ population reacts with CH_4, and the percentage of reactive ions is independent of pressure. TaC_7^+ and TaC_9^+ react completely; however, reactant ion disappearance does not exhibit a single-exponential decay. The data also do not totally fit a biexponential equation (there is a small hump), but the best fits suggest that both TaC_7^+ and TaC_9^+ have two ion populations that react at rates differing by less than a factor of 5. The rate constants given in Table III represent average values. The TaC_7^+ data suggest that one structure dominates at 80–90%, while the TaC_9^+ populations are roughly equal in abundance. Reactions of C_y^+ (y = 7–9) with D_2,[16] CH_4,[17] and HCN[18] have also revealed two structural isomers. The most reactive form (linear isomer VI) accounts for 32%, 70%, and 80% of the C_7^+, C_8^+, and C_9^+ populations, respectively.[18] Interestingly, TaC_y^+ follow this same

(34) (a) Byrd, G. D.; Burnier, R. C.; Freiser, B. S. *J. Am. Chem. Soc.* **1982**, *104*, 3565–9. (b) Byrd, G. D.; Freiser, B. S. *J. Am. Chem. Soc.* **1982**, *104*, 5944–50. (c) Huang, Y.; Wise, M. B.; Jacobson, D. B.; Freiser, B. S. *Organometallics* **1987**, *6*, 346–54. (d) Jackson, T. C.; Carlin, T. J.; Freiser, B. S. *J. Am. Chem. Soc.* **1986**, *108*, 1120–6.

(35) (a) Tolbert, M.; Beauchamp, J. L. *J. Am. Chem. Soc.* **1984**, *106*, 8117–22. (b) Tolbert, M. A.; Beauchamp, J. L. *J. Am. Chem. Soc.* **1986**, *108*, 7509–17. (c) Schilling, B. C.; Beauchamp, J. L. *Organometallics* **1988**, *7*, 194–9.

(36) (a) Sunderlin, L.; Aristov, N.; Armentrout, P. B. *J. Am. Chem. Soc.* **1987**, *109*, 78–89. (b) Sunderlin, L. S.; Armentrout, P. B. *J. Am. Chem. Soc.* **1989**, *111*, 3845–55.

(37) Irikura, K. K.; Beauchamp, J. L. *J. Am. Chem. Soc.* **1989**, *111*, 75–85.

abundance trend, with the fastest reacting fractions accounting for ~15%, 84%, and ≈50% of TaC_7^+, TaC_8^+, and TaC_9^+, respectively.

The rate trends exhibited in TaC_y^+ reactions with D_2 are also seen in reactions with CH_4. TaC_y^+ (y = 5, 11–14) react with CH_4 at rates on the order of 10^{-11}–10^{-12} cm^3/s. This is slow relative to the Langevin collision rate[32] of 9.7×10^{-10} cm^3/s. These slow reactions were not monitored to completion; however, in all cases the majority of the ions did react.

Primary Reactions with $^{13}CH_4$. In order to gain structural and mechanistic information, the reactions of $Ta^{12}C_y^+$ with $^{13}CH_4$ were studied. Experimental and statistical branching ratios for C_2H_2 elimination (reactions 13 and 14) are shown in Table IV. Sta-

$$Ta^{12}C_y^+ + {}^{13}CH_4 \rightarrow Ta^{12}C_{y-1}H_2^+ + {}^{12}C^{13}CH_2 \quad (13)$$

$$Ta^{12}C_y^+ + {}^{13}CH_4 \rightarrow Ta^{12}C_{y-2}{}^{13}CH_2^+ + {}^{12}C_2H_2 \quad (14)$$

tistical calculations assume that all carbons have an equal probability of being incorporated into the neutral C_2H_2 lost in the reaction. For y = 5, 11, and 13, the TaC_y^+ reactions with $^{13}CH_4$ are very slow relative to reaction 15 with background water

$$TaC_y^+ + H_2O \rightarrow TaC_{y-1}H_2^+ + CO \quad (15)$$

(present at ~10^{-9} Torr). As a result, the majority of $Ta^{12}C_{y-1}H_2^+$ (y = 5, 11, 13) was produced from reaction 15 and not the desired reaction with $^{13}CH_4$. Therefore, accurate branching ratios could not be determined for these ions. The other TaC_y^+ underwent reaction 15 to varying degrees, but the contribution of this process to $Ta^{12}C_{y-1}H_2^+$ intensity either was negligible or could be subtracted out. This subtraction process involved $Ta^{12}C_{y-1}H_2^+$ produced from H_2O present with the vacuum system maintained at its base pressure of ~3×10^{-9} Torr. The $Ta^{12}C_{y-1}H_2^+$ intensity reported for several $Ta^{12}C_y^+$ that are slow to react with $^{13}CH_4$ (i.e., y = 9, 13, and 14) may be slightly high due to reactions with H_2O introduced into the vacuum system with $^{13}CH_4$.

While one might expect that the reactions of TaC_y^+ with $^{13}CH_4$ would result in the preferential loss of $^{12}C^{13}CH_2$, it is evident from the data in Table III that this does *not* occur. In fact, the labeled carbon is almost *totally scrambled*; that is, each carbon in the reaction intermediate has an equal probability of being incorporated into the eliminated neutral. This indicates that the mechanism involves assimilation of the ^{13}C into the $^{12}C_y$ ligand(s). The first step is probably Ta^+ insertion into a ^{13}C–H bond, yielding intermediate XII. This is followed by one (or more) α-hydrogen

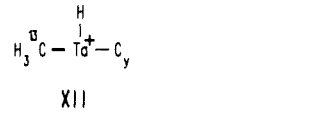

XII

migrations onto Ta^+, with some production and elimination of H_2 (reaction 10). (Although α-hydride shifts are less common in the gas phase than β-hydride shifts, they have been observed in organotantalum solution chemistry.[38]) The ^{13}C is then incorporated into $^{12}C_y$, and the excess internal energy generated by the formation of this complex results in the loss of C_2H_2.

The observation of complete scrambling may indicate that all carbons are in equivalent environments in the intermediate preceding C_2H_2 loss. Therefore, metallocene intermediates (i.e., hydrogenated versions of IV) are strong candidates, although species with multiple C_2 ligands surrounding the metal (II) cannot be ruled out. For other structures, total carbon scrambling requires that either (1) ^{13}C inserts randomly into any position in the carbon system and C_2H_2 elimination occurs at either a fixed position(s) or an indiscriminate one or (2) ^{13}C inserts in a specific location(s) but carbon incorporation into C_2H_2 is random. Intermediates similar to metallacycle V meet either requirement. Intermediates involving singular attachment of Ta^+ to a carbon chain (I or III) are less plausible because indiscriminate ^{13}C insertion (option 1) should become difficult with increasing chain length (unless the chain is severely bent) and random C–C cleavage during C_2H_2 formation (option 2) is impossible because this would result in loss of various lengths of the carbon chain. Note that it is likely that the intermediate following ^{13}C integration into C_y has the same structural type as the reactant TaC_y^+. This is not mandatory, however, since in solution Ta–alkylidene complexes (linear structures) have been known to undergo cyclometalation during reactions with hydrocarbons.[39,40]

Carbon scrambling is much more extensive with TaC_y^+ and $^{13}CH_4$ than in the corresponding C_y^+ reactions. For C_y^+ (y = 4–9) the abundance of $^{12}C^{13}CH_2$ loss is roughly 2 times greater than would be expected if total carbon scrambling occurred (e.g., C_6^+ eliminates 54% $^{12}C^{13}CH_2^+$ and 46% $^{12}C_2H_2$, while the statistical ratios of these products are 29% and 71%, respectively).[41] The proposed mechanism for C_y^+ reactions, which involves reaction at terminal carbene ends of linear chains (VI),[16-18] should not yield a high degree of carbon scrambling. The total scrambling seen for TaC_y^+ is further evidence that these processes do not involve a similar mechanism.

The reactions of TaC_y^+ and $^{13}CH_4$ also indicate the presence of labile hydrogens; that is, hydrogens that do not remain attached to ^{13}C. As additional confirmation, H/D exchange reactions were employed to indicate Ta^+–H character. $TaC_yH_2^+$ (y = 2–5) readily undergo two sequential H/D exchanges with D_2. The rate of exchange decreases as the number of carbons increases, with no exchanges observed for $y \geq 6$. Assuming that D_2 initially inserts at the metal forming two Ta^+–D bonds, these data signify that the $TaC_yH_2^+$ hydrogens reside either on Ta^+ or in equilibrium between Ta^+ and carbon-containing ligands. The lack of H/D exchange for $y \geq 6$ does not necessarily imply a lack of labile hydrogens. Instead, D_2 may not oxidatively add to these species, possibly as a result of coordinative saturation.

Secondary Reactions. $TaC_yH_2^+$ (y = 1–6) produced from the reactions of TaC_y^+ and CH_4 readily react with a second neutral molecule. Dehydrogenation, reaction 16, is the only process observed and occurs at rates on the order of 10^{-10}–10^{-11} cm^3/s.

$$TaC_yH_2^+ + CH_4 \rightarrow TaC_{y+1}H_4^+ + H_2 \quad (16)$$

These processes are independent of the TaC_y^+ primary reactant; for example, $TaC_2H_2^+$ produced from TaC^+ (by loss of H_2) and from TaC_3^+ (by loss of C_2H_2) react in an identical manner. Larger $TaC_yH_2^+$ (y = 7–13) do not react with CH_4. Aside from adduct formation for y = 9, 11, and 13, these ions also do not react (or H/D exchange) with D_2, while TaC_y^+ (y = 7–13) react with both D_2 and CH_4. This may indicate that the hydrogens of $TaC_yH_2^+$ occupy coordination sites on Ta^+ and block any further oxidative addition processes. It is also possible, although less likely, that hydrogenation of C_y results in a more dramatic change in structure, leading to multiple carbon ligands that hinder subsequent oxidative addition.

The reaction of $TaC_2H_2^+$ with CH_4 is 1 order of magnitude slower than the other $TaC_yH_2^+$ reactions. The product ion, $TaC_3H_4^+$, does not react further with CH_4. Upon collisional activation, $TaC_3H_4^+$ eliminates predominantly H_2 at low energies (reaction 17) and C_2H_2 at higher energies (reaction 18). Since

$$TaC_3H_4^+ \rightarrow TaC_3H_2^+ + H_2 \quad (17)$$

$$TaC_3H_4^+ \rightarrow TaCH_2^+ + C_2H_2 \quad (18)$$

$TaCH_2^+$ and $TaC_2H_2^+$ both dissociate to produce primarily Ta^+, with no H_2 elimination, the facile loss of H_2 from $TaC_3H_4^+$

(38) (a) van Asselt, A.; Burger, B. J.; Gibson, V. C.; Bercaw, J. E. *J. Am. Chem. Soc.* **1986**, *108*, 5347–9. (b) Chamberlain, L. R.; Rothwell, I. P. *J. Chem. Soc., Dalton Trans.* **1987**, 163–7. (c) Malatesta, V.; Ingold, K. U.; Schrock, R. R. *J. Organomet. Chem.* **1978**, *152*, C53–6.

(39) (a) Steffey, B. D.; Chamberlain, L. R.; Chesnut, R. W.; Chebi, D. E.; Fanwick, P. E.; Rothwell, I. P. *Organometallics* **1989**, *8*, 1419–23. (b) Chesnut, R. W.; Steffey, B. D.; Rothwell, I. P.; Huffman, J. C. *Polyhedron* **1988**, *7*, 753–6.

(40) (a) Fellmann, J. D.; Schrock, R. R.; Rupprecht, G. A. *J. Am. Chem. Soc.* **1981**, *103*, 5752–8. (b) McLain, S. J.; Schrock, R. R. *J. Am. Chem. Soc.* **1978**, *100*, 1315–7.

(41) McElvany, S. W. Unpublished results.

Table V. Branching Ratios and Normalized Rate Constants for the Primary Reactions of TaC_y^+ and C_2H_4

	cluster size (y)														
products	0	1	2	3	4	5	6	7	8	9	10	11	12	13	14
$TaC_{y+2}H_2^+ + H_2$	1.00	0.24	0.60	0.28	0.72	0.18	0.36		0.68	0.11	0.40		0.63	0.26	0.26
$TaC_3H^+ + 3H$		0.11													
$TaC_3^+ + 2H_2$		0.22													
$TaC_yH_2^+ + C_2H_2$		0.27	0.40	0.72	0.28	0.82	0.64	1.00	0.32	0.89	0.60	1.00	0.37	0.74	0.74
$TaCH^+ + C_2H_3$		0.05													
$Ta^+ + C_3H_4$		0.11													
normalized rate const (k_p)	1.00[a]	1.19	0.93	0.80	0.74	0.55	0.82	0.74	0.58	0.67	0.83	0.47	0.45	0.079[b]	0.26[b]

[a] The absolute rate constant for the reaction of Ta^+ was estimated to be 1.1×10^{-9} cm^3/s. [b] See text for explanation.

Table VI. Branching Ratios for the Loss of $^{13}C_2D_2$, $^{12}C^{13}CD_2$, and $^{12}C_2D_2$ in the Reactions of $Ta^{13}C_y^+$ and $^{12}C_2D_4$

	cluster size (y)										
products	2	3	4	5	6	7	8	9	10	11	12
$Ta^{12}C_2{}^{13}C_{y-2}D_2^+ + {}^{13}C_2D_2$											
exptl	0.17	0.24	0.25	0.58	0.52	0.49	0.51	0.49	0.64	0.61	0.71
stat[a]	0.17	0.30	0.40	0.48	0.53	0.58	0.62	0.65	0.68	0.71	0.73
$Ta^{12}C_1{}^{13}C_{y-1}D_2^+ + {}^{12}C^{13}CD_2$											
exptl	0.59	0.69	0.64	0.33	0.37	0.45	0.39	0.42	0.30	0.34	0.28
stat[a]	0.66	0.60	0.53	0.48	0.43	0.39	0.36	0.33	0.30	0.28	0.26
$Ta^{13}C_yD_2^+ + {}^{12}C_2D_2$											
exptl	0.24	0.07	0.12	0.09	0.11	0.06	0.10	0.09	0.06	0.05	0.00
stat[a]	0.17	0.10	0.07	0.05	0.04	0.03	0.02	0.02	0.02	0.01	0.01

[a] Statistical calculations of branching ratios assume that all carbons have an equal probability of being incorporated in the neutral C_2D_2. The statistical abundance of $Ta^{12}C_2{}^{13}C_{y-2}D_2^+$ is $[y(y-1)]/[(y+1)(y+2)]$, of $Ta^{12}C_1{}^{13}C_{y-1}D_2^+$ is $(4y)/[(y+1)(y+2)]$, and of $Ta^{13}C_nD_2^+$ is $2/[(y+1)(y+2)]$.

suggests that ligand coupling has occurred, yielding a Ta^+–(C_3H_4) structure rather than a carbene–olefin complex, (CH_2)–Ta^+–(C_2H_2).

Several product ions from reaction 16 also dehydrogenate CH_4. For example, Ta^+ initiates four sequential reactions with CH_4. Low-energy CID of the product ions $TaC_2H_4^+$, $TaC_3H_6^+$, and $TaC_4H_8^+$ results in elimination of H_2 and small hydrocarbons but does not yield conclusive structural information.[21] TaC_2^+ also dehydrogenates four CH_4 molecules, producing $TaC_{n+2}H_{2n}^+$ (n = 1–4). The tertiary product, $TaC_4H_4^+$, dissociates by elimination of H_2 at lower CID energies, C_2H_2 at moderate energies, and C_4H_4 at higher energies. Interestingly, the C_2H_2 loss pathway exhibited near-statistical carbon scrambling during CID studies of $Ta^{12}C_2{}^{13}C_2H_4^+$. $TaC_4H_2^+$, the TaC_3^+ and CH_4 product ion, dehydrogenates CH_4 to produce $TaC_5H_4^+$, which then reacts slowly by association to yield $TaC_6H_8^+$. This is the only adduct formation seen for the CH_4 reactions. Surprisingly, dehydrogenation to form $TaC_6H_6^+$ (which may have a stable Ta^+–benzene structure) is not observed.

Ethene Reactions. Primary Reactions. Primary products, branching ratios, and rate constants for the reactions of TaC_y^+ with C_2H_4 are listed in Table V. Two pathways dominate these reactions. Elimination of H_2 (reaction 19) results in an increase in the number of carbons attached to the metal, while acetylene elimination (reaction 20) does not change the number of carbons.

$$TaC_y^+ + C_2H_4 \rightarrow TaC_{y+2}H_2^+ + H_2 \quad (19)$$

$$TaC_y^+ + C_2H_4 \rightarrow TaC_yH_2^+ + C_2H_2 \quad (20)$$

Two superimposed trends are evident from the data: C_2H_2 elimination becomes more prevalent as the number of carbons increases, and TaC_y^+ with even number of carbons preferentially lose H_2. The reactivity of TaC^+ is again unusual and involves additional processes resulting in 3 H, 2 H_2, C_2H_3, and C_3H_4 elimination. The exothermic loss of 2 H_2 to generate TaC_3^+ indicates that the Ta^+–C_3 bond is at least 16 kcal/mol stronger than the Ta^+–C bond.[29] This is consistent with the D_2 reaction data and also with the DLV production of TaC^+ in much lower abundance than TaC_3^+.

The rates of the TaC_y^+ (y = 0–12) reactions with C_2H_4 range from 7 to 13×10^{-10} cm^3/s, suggesting that every first or second collision results in reaction. For y = 0–2, the measured rates are slightly higher than the collision rate[32] of 9.8×10^{-10} cm^3/s, indicating that the absolute rates obtained from our experiments are somewhat high. However, as noted previously, differences in relative rate constants should be significant since data were obtained under similar conditions. The fast reactions of TaC_y^+ (y = 0–12) with C_2H_4 result in relative rates that vary by less than a factor of 3 and that do not exhibit the pronounced trends seen with D_2 and CH_4. These ion populations react completely with C_2H_4, showing only pseudo-first-order kinetic behavior. This indicates that the two structural isomers of TaC_y^+ (y = 7–9) have similar reactivities with C_2H_4. The linear and cyclic forms of C_y^+ (y = 7–9) also cannot be distinguished by reaction with C_2H_4.[17] TaC_{13}^+, and to a lesser extent TaC_{14}^+, reacts more slowly than the other cluster ions. These processes were not monitored to completion, but in both instances greater than 70% reaction was observed.

The reactions of TaC_y^+ and C_2H_4 are dramatically different from those of the corresponding C_y^+. C_y^+ (y = 3–14) react with C_2H_4 via nine pathways, including adduct formation, charge exchange (formation of neutral C_y), and elimination of H, H_2, CH_3, C_2H_2, C_3H_3, C_4H_2, and $C_{y-1}H$. The proposed mechanism involves insertion of the carbene ends of linear C_y^+ into both the C—H and C=C bonds of C_2H_4.[17] Again, differences in TaC_y^+ and C_y^+ reactivities indicate active participation of Ta^+ in the TaC_y^+ reactions.

$^{12}C_2D_4$ Reactions with $Ta^{13}C_y^+$. To aid in the elucidation of mechanisms, the reactions of $Ta^{13}C_y^+$ with $^{12}C_2D_4$ were investigated. These experiments were performed with $^{12}C_2D_4$ rather than $^{12}C_2H_4$ to avoid nominal mass overlap between $Ta^{13}C_y^+$ and $Ta^{12}C_2{}^{13}C_{y-1}H_2^+$. DLV on a Ta/^{13}C (amorphous) samples did not yield sufficient $Ta^{13}C^+$ for further study, while low ion intensities hindered work with $Ta^{13}C_{13}^+$ and $Ta^{13}C_{14}^+$. Experimental and statistical branching ratios for C_2D_2 elimination (reactions 21–23) are given in Table VI. Statistical calculations do not

$$Ta^{13}C_y^+ + {}^{12}C_2D_4 \rightarrow Ta^{12}C_2{}^{13}C_{y-2}D_2^+ + {}^{13}C_2D_2 \quad (21)$$

$$Ta^{13}C_y^+ + {}^{12}C_2D_4 \rightarrow Ta^{12}C^{13}C_{y-1}D_2^+ + {}^{12}C^{13}CD_2 \quad (22)$$

$$Ta^{13}C_y^+ + {}^{12}C_2D_4 \rightarrow Ta^{13}C_yD_2^+ + {}^{12}C_2D_2 \quad (23)$$

consider that the two ^{12}C's may reside in adjacent sites in the reaction intermediate. While the degree of carbon scrambling is not as great as that seen with $^{13}CH_4$, it is still extensive and suggests that the ^{12}C's from $^{12}C_2D_4$ are being incorporated into the $^{13}C_y$ ligand(s) prior to C_2D_2 elimination. Also, the enhanced $^{12}C_2D_2$ elimination over statistical expectations implies that a minor

amount of neutral elimination occurs prior to incorporation of $^{12}C_2$ into $^{13}C_y$.

A goal of the $Ta^{13}C_y^+$ and $^{12}C_2D_4$ study was to gain structural information. With $Ta^{13}C_7^+$ as an example, insertion of intact $^{12}C_2$ into the cyclic $^{13}C_7$ ligand of a metallocene (IV) followed by elimination of any two adjacent carbon atoms would theoretically result in the distribution of $^{13}C_2D_2$, $^{12}C^{13}CD_2$, and $^{12}C_2D_2$ elimination being 67%, 22%, and 11%, respectively. Insertion of an intact $^{12}C_2$ next to Ta^+ in a metallacycle (V) or linear $^{13}C_7$ chain (I) with elimination of any adjacent C_2 would result in a distribution of 75%, 12.5%, and 12.5%, while insertion at any site in these structures yields 66%, 22%, and 12%. Unfortunately, the experimental product distributions of 49%, 45%, and 6% cannot be explained with these simple models. In fact, the experimental data most closely match the statistical distribution from complete carbon scrambling (58%, 39%, 3%), although a greater tendency toward ^{12}C elimination is seen experimentally. The agreement between the experimental data and the statistical distribution suggests that the two ^{12}C's from $^{12}C_2D_4$ may not be adjacent in the intermediate. Therefore, the reaction may involve some initial insertion of Ta^+ into the C=C bond. However, the abundance of the dehydrogenation pathway (reaction 20) illustrates that Ta^+ insertion into the vinylic C–H bond is the major process. In addition, a strong preference for C–H insertion over C–C insertion has been observed for the reactions of Ta^+ with hydrocarbons.[21]

Secondary Reactions. Activation of C–H bonds governs the reactions of $TaC_mH_n^+$ with C_2H_4. Typically, smaller clusters increase in size by retaining C_2H_2 (reaction 24), while larger clusters retain H_2 (reaction 25). Double dehydrogenation (reaction 26) occurs to a surprising degree and is more pronounced as the length of the carbon chain increases. The extent of these secondary reactions is truly extraordinary and appears to involve coupling of hydrocarbon ligands on the metal. Ligand coupling is also observed in the gas-phase reactions of Nb^+ with hydrocarbons[21] and in solution-phase organotantalum chemistry, where polymerization of unsaturated hydrocarbons is proposed to proceed through insertion,[42] metathesis,[43] and cyclometalation[40] mechanisms.

$$TaC_mH_n^+ + C_2H_4 \rightarrow TaC_{m+2}H_{n+2}^+ + H_2 \quad (24)$$
$$\rightarrow TaC_mH_{n+2}^+ + C_2H_2 \quad (25)$$
$$\rightarrow TaC_{m+2}H_n^+ + 2H_2 \quad (26)$$

Ta^+ sequentially reacts with *10* C_2H_4 molecules. This is the most extensive reactivity ever observed in gas-phase metal ion chemistry, eclipsing the reaction of Nb^+ with six C_2H_4 molecules.[44] The primary product from Ta^+ and C_2H_4, $TaC_2H_2^+$, undergoes secondary reactions 27 and 28 at 20% and 80%, respectively.

$$TaC_2H_2^+ + C_2H_4 \rightarrow TaC_4H_2^+ + 2H_2 \quad (27)$$
$$\rightarrow TaC_4H_4^+ + H_2 \quad (28)$$

Further reactions were not studied in detail with ion isolation techniques; therefore, accurate branching ratios and rate constants were not obtained for each step. However, elimination of a single H_2 controls the subsequent reactions with four additional C_2H_4 molecules, resulting in the sequential formation of $TaC_nH_{n-2}^+$ and $TaC_nH_n^+$ (n = 6, 8, 10, 12). $TaC_nH_n^+$ also eliminate a minor amount of 2 H_2, but 2 H_2 loss does not occur for the more unsaturated $TaC_nH_{n-2}^+$. These processes proceed readily, at rates on the order of 10^{-10} cm^3/s, with $TaC_nH_{n-2}^+$ reacting faster than the corresponding $TaC_nH_n^+$. Following the formation of $TaC_{12}H_{10}^+$ and $TaC_{12}H_{12}^+$, the rates decrease by roughly 1 order of magnitude. The next set of reactions in the sequence involve 2 H_2 elimination, forming $TaC_{14}H_{10}^+$ and $TaC_{14}H_{12}^+$. The rate of reaction again slows significantly, but processes involving H_2 and 2 H_2 loss continue and terminate in the formation of $TaC_{20}H_n^+$ (n = 14, 16, 18). No additional reactions were observed, even with the introduction of relatively high pressures ($\sim 10^{-3}$ Torr) of C_2H_4 via the pulsed valve.

$TaC_2H_2^+$ produced from TaC_2^+ and C_2H_4 reacts in a manner identical with $TaC_2H_2^+$ formed by Ta^+ reaction with C_2H_4. The major TaC_2^+ primary product, $TaC_4H_2^+$, reacts further with the neutral by H_2 elimination, yielding $TaC_6H_4^+$. The sequence then continues in the manner outlined above for Ta^+, again concluding with the generation of $TaC_{20}H_n^+$. In addition, CID studies of several $TaC_mH_n^+$ produced from reactions initiated by both Ta^+ and TaC_2^+ suggest that the product ion structures are independent of the initial TaC_y^+ reactant.

Collision-induced dissociation of $TaC_mH_n^+$ typically yields a large number of products and involves elimination of H_2 and small hydrocarbons containing even numbers of carbons. For $TaC_{14}H_{12}^+$, $TaC_{12}H_{12}^+$, $TaC_{12}H_{10}^+$, and $TaC_{10}H_8^+$, the major low-energy processes are H_2 or C_2H_2 loss, with elimination of 2 H_2 and C_2H_4 (or C_2H_2 and H_2) resulting at moderately higher energies. As the CID energy is increased, a series of lower mass ions form: $TaC_8H_6^+$, $TaC_6H_4^+$, $TaC_4H_2^+$, $TaC_2H_2^+$, Ta^+. These same ions are produced regardless of the dissociating $TaC_mH_n^+$, indicating that dissociation is governed by the stability of the product ions rather than the neutrals.

$TaC_6H_6^+$ formed by reactions of Ta^+ (or TaC_2^+) with C_2H_4 readily dissociates under low-energy conditions. $TaC_6H_6^+$, which is produced from cyclohexane and presumably has a Ta^+–benzene structure, yields the same CID products but in different relative abundances. Reactions 29–33 show these products at 15-eV laboratory energy with xenon collision gas. At higher CID energies, hydrocarbon elimination (reactions 31–33) increases relative to dehydrogenation (reactions 29 and 30). $TaC_6H_6^+$ from C_2H_4 undergoes considerably more 2 H_2 loss at all energies studied than $TaC_6H_6^+$ from cyclohexane. In fact, with cyclohexane as the precursor, reaction 30 never accounts for greater than 3% of the CID products. Ions produced from different pathways, but having identical structures, can exhibit variations in their dissociation patterns as a result of differences in initial internal energies. However, for $TaC_6H_6^+$ generated from C_2H_4 and cyclohexane the discord in the CID data is sufficient to suggest that these ions do not have the same structure. A linear hydrocarbon chain should dehydrogenate more readily than a benzene ring; therefore, benzene formation (e.g., dehydrocyclization) is probably not occurring in the C_2H_4 reactions. In contrast, $NbC_6H_6^+$ produced from C_2H_4 (in a reaction sequence analogous to that of Ta^+) and from cyclohexane dissociates to generate the same CID fragments in roughly the same intensities, leading to the conclusion that Nb^+ reacts sequentially with C_2H_4 to yield Nb^+–benzene.[21]

precursor		C_2H_4	c-C_6H_{12}	
$TaC_6H_6^+$	$\rightarrow TaC_6H_4^+ + H_2$	37%	63%	(29)
	$\rightarrow TaC_6H_2^+ + 2H_2$	24	2	(30)
	$\rightarrow TaC_4H_2^+ + C_2H_4$	13	17	(31)
	$\rightarrow TaC_2H_2^+ + C_4H_4$	10	4	(32)
	$\rightarrow Ta^+ + C_6H_6$	16	14	(33)

$TaC_{12}H_{12}^+$ produced by reactions of Ta^+ with C_2H_4 and with cyclohexane and cyclohexene (both probably yielding Ta^+–dibenzene) dissociate via 10 pathways. Again, variations in relative CID product abundances are seen and may imply different $TaC_{12}H_{12}^+$ structures. This cannot be said with certainty, because these differences are minor and may again result from variations in initial internal energy of the dissociating ions. Interestingly, $TaC_{12}H_{12}^+$ does not dissociate to form $TaC_6H_6^+$. Also, $TaC_6H_6^+$ was not produced as a CID product from any $TaC_mH_n^+$ species studied. In contrast, $NbC_8H_8^+$ and $NbC_{12}H_{12}^+$ (formed from Nb^+

(42) (a) Wallace, K. C.; Liu, A. H.; Davis, W. M.; Schrock, R. R. *Organometallics* **1989**, *8*, 644–54. (b) Wallace, K. C.; Schrock, R. R. *Macromolecules* **1987**, *20*, 448–50.

(43) (a) Wallace, K. C.; Liu, A. H.; Dewan, J. C.; Schrock, R. R. *J. Am. Chem. Soc.* **1988**, *110*, 4964–77. (b) Wood, C. D.; McLain, S. J.; Schrock, R. R. *J. Am. Chem. Soc.* **1979**, *101*, 3210–22. (c) Rocklage, S. M.; Fellmann, J. D.; Rupprecht, G. A.; Messerle, L. W.; Schrock, R. R. *J. Am. Chem. Soc.* **1981**, *103*, 1440–7.

(44) The reactions of Nb^+ and C_2H_4 reported in ref 21 were performed at static pressures of $\sim 10^{-7}$ Torr. It is possible that Nb^+ might also react with greater than six C_2H_4 molecules at the higher pressures (both static and pulsed) employed in the present TaC_y^+ study.

Table VII. Branching Ratios and Normalized Rate Constants for the Primary Reactions of TaC_y^+ and C_2H_6

	cluster size (y)														
products	0	1	2	3	4	5	6	7	8	9	10	11	12	13	14
$TaC_{y+2}H_4^+ + H_2$	0.17					0.14					0.39		0.21	NR[c]	
$TaC_{y+2}H_2^+ + 2H_2$	0.80	0.57	0.64	0.18	0.26	0.35			0.82				0.56		
$TaC_{y+1}H^+ + CH_4$	0.03	0.06													
$TaC_yH_4^+ + C_2H_2$						0.16				0.49	0.21	0.27			
$TaC_yH_2^+ + C_2H_4$		0.30	0.36	0.82	0.74	0.35	1.00	1.00	0.18	0.51	0.40	0.73	0.24		1.00
$Ta^+ + C_3H_6$		0.07													
normalized rate const (k_p)	1.00[a]	0.91	0.62	0.53	0.63	0.20	0.64	0.46	0.64[b]	0.28	0.73	0.12	0.19	<0.001	0.10[d]

[a] The absolute rate constant for the reaction of Ta^+ was estimated to be 8.8×10^{-10} cm^3/s. [b] Rate constant for the reactive fraction of TaC_8^+ as discussed in the text. [c] NR indicates that this ion did not undergo any reactions. [d] See the text for explanation.

and C_2H_4) yield $NbC_6H_6^+$ as a major dissociation product.[21] $NbC_6H_6^+$ is also a major CID product for $NbC_{12}H_{12}^+$ produced from cyclohexane, but differences in the CID product intensities for $NbC_{12}H_{12}^+$ from the two precursors prevent unambiguous structural assignment. However, ligand coupling to avoid coordinative saturation and dehydrocyclization producing benzene ligands are believed to be prominent processes in the Nb^+/ethene chemistry.[21] While ligand coupling appears to be prevalent in the Ta^+ reactions, there is currently no evidence for dehydrocyclization. In addition, M^+–benzene bonds are generally strong relative to other M^+–alkene bonds.[45] The apparent lack of Ta^+–benzene formation may indicate that this is not the case for Ta.

In addition to Ta^+ and TaC_2^+, the other TaC_y^+ also undergo complex series of reactions with ethene. The TaC^+ secondary reactions were difficult to study due to the low TaC^+ intensity and the large number (six) of primary products, but subsequent products up to $TaC_9H_8^+$ were observed. The TaC_3^+ primary products, $TaC_3H_2^+$ and $TaC_5H_2^+$, react predominantly by loss of H_2 and 2 H_2 to form two series of ions, $TaC_nH_{n-3}^+$ and $TaC_nH_{n-1}^+$ (n = 5, 7, 9, 11). Both n = 11 ions then produce $TaC_{13}H_{10}^+$. Following the trend of the Ta^+ reactions, the more unsaturated series, $TaC_nH_{n-3}^+$, reacts the fastest. The TaC_4^+ products, $TaC_4H_2^+$ and $TaC_6H_2^+$, form the secondary products $TaC_6H_4^+$ and $TaC_8H_4^+$. Interestingly, although $TaC_8H_4^+$ is relatively unsaturated, it undergoes only a very slow reaction to yield $TaC_{10}H_6^+$. In contrast, $TaC_6H_4^+$ readily continues a sequence of H_2 eliminations that concludes in the production of $TaC_{14}H_{12}^+$. TaC_5^+ initiates a complicated series of reactions involving product ions with both odd and even numbers of hydrogens. These reactions terminate in the formation of $TaC_{13}H_n^+$ (n = 8–12), with n = 8 dominating. The primary products from TaC_6^+, $TaC_6H_2^+$ and $TaC_8H_2^+$, react by both C_2H_2 and H_2 elimination and eventually produce $TaC_{12}H_6^+$. (Again, $TaC_8H_4^+$ is slow to react.) $TaC_7H_2^+$, from TaC_7^+, produces $TaC_7H_4^+$, $TaC_9H_4^+$, $TaC_9H_6^+$, and $TaC_{11}H_6^+$. Elimination of C_2H_2 to form $TaC_yH_4^+$ is the only process observed for $TaC_yH_2^+$ (y = 8–13), which are originally produced from the corresponding TaC_y^+. An interesting aspect of the secondary reactions is that the rate of reaciton drops considerably after the formation of $TaC_{13}H_n^+$ or $TaC_{14}H_n^+$ species. TaC_y^+ formation by DLV also drops off considerably between y = 14 and 15. One possibility is that Ta forms several bonds with the hydrocarbon ligand(s) and coordinative saturation may hinder ligands with more than a total of 14 carbons.

Ethane Reactions. Primary Reactions. As seen in Table VII, the reactions of TaC_y^+ and C_2H_6 involve six different processes. Two major pathways, elimination of 2 H_2 (reaction 34) and C_2H_4 (reaction 35), are observed. Interestingly, these reactions lead

$$TaC_y^+ + C_2H_6 \rightarrow TaC_{y+2}H_2^+ + 2H_2 \quad (34)$$

$$TaC_y^+ + C_2H_6 \rightarrow TaC_yH_2^+ + C_2H_4 \quad (35)$$

to the same products that are produced from TaC_y^+ reactions with C_2H_4 (via H_2 and C_2H_2 loss). $TaC_{y+2}H_2^+$ production from C_2H_6 (reaction 34) requires 32 kcal/mol more energy than its production from C_2H_4 (reaction 19). In contrast, formation of $TaC_yH_2^+$ from C_2H_6 (reaction 35) needs 9 kcal/mol less energy than the corresponding C_2H_4 reaction (reaction 20).[29] Again, dehydrogenation to increase the carbon to Ta ratio becomes less important with increasing y but is more pronounced for even y. Loss of H_2 and C_2H_2 from ethane is most prevalent at larger y ($y \geq 9$). Ta^+ and TaC^+ eliminate a minor amount of CH_4, probably as a result of oxidative addition of the metal into the C–C bond.

The TaC_y^+ (y = 0–4, 6–10) reactions with C_2H_6 are less than a factor of 2 slower than the corresponding C_2H_4 reactions. For y = 5 and 11–14, the C_2H_6 reactions are considerably slower than those of C_2H_4. Similar behavior is found with D_2 and CH_4. Only 84% of the TaC_8^+ population reacts with C_2H_6, providing additional evidence for two TaC_8^+ structures. TaC_{13}^+, which reacts very slowly with C_2H_4, does not react with C_2H_6. The TaC_{14}^+ reaction was not monitored to completion, but at least 70% of the ions react. All other TaC_y^+ react completely with C_2H_6 and exhibit only pseudo-first-order kinetic behavior.

Secondary Reactions. The primary product ions formed from TaC_y^+ and C_2H_6 react extensively with C_2H_6. These reactions were not studied in detail due to the extreme complexity of the spectra. In general, elimination of H_2 and 2 H_2 is the major secondary processes, with H_2 loss becoming more important as the length of the carbon chain increases. C_2H_2 and C_2H_4 eliminations also occur, as well as minor amounts of CH_4 loss. The secondary reactivity of the $TaC_mH_n^+$ product ions again decreases as the number of carbons increases, and no ions larger than m = 14 are observed.

Conclusions

Tantalum carbide cluster ions, TaC_y^+ (y = 0–14), exhibit a rich chemistry in their gas-phase reactions with D_2, CH_4, C_2H_4, and C_2H_6. These processes are markedly different from those of the corresponding carbon clusters, C_y^+,[16,17] indicating that Ta is playing an active role in the TaC_y^+ reactions. The reaction mechanisms are believed to involve oxidative addition at Ta^+, followed by ligand rearrangement and elimination of neutrals or radicals. The high degree of dehydrogenation and ligand coupling seen in gas-phase Ta^+ chemistry[21] is also found in the TaC_y^+ reactions with hydrocarbons. In addition, the TaC_y^+ reactions with hydrocarbons mimic Ta^+ chemistry by undergoing extensive secondary reactions. For example, Ta^+ and TaC_2^+ react sequentially with ten and nine C_2H_4 molecules, respectively, leading to the formation of large ions such as $TaC_{20}H_{18}^+$.

Experiments with isotopically labeled precursors were performed to obtain structural and mechanistic information. Surprisingly, total scrambling of the labeled carbon occurred during TaC_y^+ reactions with $^{13}CH_4$. This indicates that the mechanism involves assimilation of the ^{13}C into the $^{12}C_y$ ligand(s) prior to neutral elimination. As additional confirmation, extensive carbon scrambling was also observed during $Ta^{13}C_y^+$ reactions with C_2D_4.

Direct evidence for TaC_y^+ structures was not obtained from the reactivity studies. However, the observation of complete carbon scrambling in the $^{13}CH_4$ reactions suggests an intermediate with all carbons in equivalent environments (e.g., metallocene structures). Previous low-energy CID studies[13] of TaC_y^+ have also indicated the possibility of cyclic structures, particularly for $y \geq 10$. In addition, the reactions of TaC_y^+ (y = 7–9) with D_2 and CH_4 provide evidence for two structural isomers.

(45) Hettich, R. L.; Jackson, T. C.; Stanko, E. M.; Freiser, B. S. *J. Am. Chem. Soc.* **1986**, *108*, 5086–93.